

Charge localization and stripes in a two-dimensional three-band Peierls-Hubbard model

Z. G. Yu, J. Zang, J. T. Gammel, and A. R. Bishop

Theoretical Division, Los Alamos National Laboratory, Los Alamos, New Mexico 87545

(Received 12 September 1997)

Using a two-dimensional three-band Peierls-Hubbard model appropriate to layered transition-metal oxides, and in an inhomogeneous Hartree-Fock approximation, we show that several kinds of charge-localized mesoscopic patterns (stripes) may exist: vertical site stripes, vertical zig-zag stripes, diagonal site stripes, and oxygen-centered stripes. A random-phase-approximation analysis reveals new phonon modes and intense low-energy spin excitations in these stripes. A softened phonon mode with momentum $(\pi, 0)$ in the oxygen-centered stripe may explain the anomalous phonons observed by neutron-scattering experiments in several cuprate superconductors. [S0163-1829(98)50210-X]

Charge localization (small polaron formation) has been observed in recent years in a variety of doped transition-metal oxides including nickelates, cuprates, and manganites, and the organization of the localized holes into mesoscopic patterns, particularly “stripes,” has been suggested. For example, neutron-scattering experiments have shown that in $\text{La}_{1.48}\text{Nd}_{0.4}\text{Sr}_{0.12}\text{CuO}_4$, doped holes form commensurate charge-localized stripes.^{1,2} These stripes are also antiphase domain walls between antiferromagnetically ordered spins in the CuO_2 planes, and simultaneously, the superconductivity is suppressed.^{1,2} This observation may imply that stripes are important for the physics of high-temperature superconductors, and the excitations of spin, charge, and lattice with respect to them are therefore of central interest. Several theoretical studies suggest that stripes may have significant impact on the superconductivity in cuprates.³⁻⁷ Theoretically, the stripe phase has been predicted by solving the Hubbard model or the t - J model in the Hartree-Fock (HF) approximation,⁸⁻¹¹ and by numerical density matrix renormalization group (DMRG) calculations for the t - J model.¹² However, these calculations have not considered the freedom of oxygen sites, which has been shown to be one important factor for stabilizing stripes.¹³ Recent measurements also suggest that stripes may occupy the oxygen (rather than transition-metal) sites (bond stripes).^{14,15} Very recent inelastic neutron scattering experiments on $\text{La}_{1.85}\text{Sr}_{0.15}\text{CuO}_4$ suggest that a phonon mode with momentum $(\pi, 0)$ becomes softened and localized possibly due to the formation of bond stripes.¹⁴ (Evidence for related anomalous phonons exists in several layered cuprates.¹⁶)

For a systematic understanding of, and discrimination between, various charge-ordered patterns in transition-metal oxides, it will be necessary to characterize both electronic energy scale (pseudogap regime) and low-energy vibrational modes (of lattice, charge and spin)—and most importantly their inter-relationships.¹⁷ To this end, here we use a two-dimensional three-band Peierls-Hubbard model, in which $d_{x^2-y^2}$ orbitals of, e.g., Cu and $p_{x,y}$ of O are explicitly included, and moreover electron-phonon (e -ph) interactions are taken into account. (A more complete model of nickelates includes an additional d orbital: Results will be given elsewhere.) The Hamiltonian of this model reads

$$\begin{aligned}
 H = & \sum_{i \neq j, \sigma} t_{ij}(\{u_k\}) c_{i\sigma}^\dagger c_{j\sigma} + \sum_{i, \sigma} e_i(\{u_k\}) c_{i\sigma}^\dagger c_{i\sigma} \\
 & + \sum_i U_i c_{i\uparrow}^\dagger c_{i\downarrow}^\dagger c_{i\downarrow} c_{i\uparrow} + \sum_{\langle i \neq j \rangle, \sigma, \sigma'} U_{ij} c_{i\sigma}^\dagger c_{j\sigma'}^\dagger c_{j\sigma'} c_{i\sigma} \\
 & + \sum_l \frac{1}{2M_l} p_l^2 + \sum_{k,l} \frac{1}{2} K_{kl} u_k u_l, \quad (1)
 \end{aligned}$$

which has been successfully employed to study the polaron states in cuprates¹⁷ and the unusual low-energy magnetic excitations in $\text{La}_2\text{Cu}_{0.5}\text{Li}_{0.5}\text{O}_4$.¹⁸ Here $c_{i\sigma}^\dagger$ creates a hole with spin σ at site i in the Cu $d_{x^2-y^2}$ or the O $p_{x,y}$ orbital. For the lattice part, we study only the motion of O ions along the Cu-O bonds and assume, for simplicity, that only diagonal components of the spring-constant matrix are finite, $K_{kl} = \delta_{kl}K$. For electron-lattice couplings, we assume that the nearest-neighbor Cu-O hopping is modified by the O-ion displacement u_k as $t_{ij} = t_{pd} \pm \alpha u_k$, where the $+$ ($-$) applies if the bond shrinks (stretches) with positive u_k . The Cu-site energy is assumed to be modulated by the O-ion displacement u_k linearly as $e_i = \epsilon_d + \beta \sum_k (\pm u_k)$, where the sum extends over the four surrounding O ions. Other forms of e -ph coupling can be easily included in our approach, as well as disorder and impurities. We include Hubbard repulsion on both Cu-site (U_d) and O-site (U_p) and the nearest-neighbor Cu-O Coulomb repulsion (U_{pd}).

Mean-field states were obtained by solving the Hamiltonian in an unrestricted HF approximation with self-consistent conditions for on-site and nearest-neighbor charge and spin densities, as well as lattice displacements, without assumption on the form of these quantities.¹⁷ Self-consistent nonlinear equations are obtained by minimizing the total energy with respect to these quantities, resulting in generally inhomogeneous patterns. We use periodic boundary conditions and the parameters are taken from local-density-approximation electronic estimates: $t_{pd} = 1$, $\Delta \equiv \epsilon_p - \epsilon_d = 4$, $U_d = 10$, $U_p = 3$, and $U_{pd} = 1$, $\alpha = 4.5/\text{\AA}$, $\beta = 1/\text{\AA}$, and $K = 32/\text{\AA}^2$.^{19,17} We choose the system in such a way that it consists of 5×4 CuO_2 unit cells for vertical stripes and 5×5 unit cells for diagonal stripes. Since the stripe is an antiphase antiferromagnetic domain wall, in such systems mismatch of

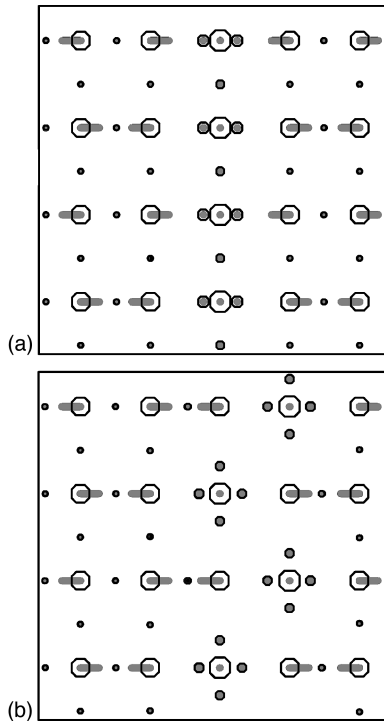


FIG. 1. Charge (radii of the circles) and spin (arrows) densities in the vertical site stripe (a) and zig-zag stripe (b). The large circles are for Cu sites and the small ones for O sites. The hole concentration is 0.2.

spin in the boundary can be avoided. We add four extra holes to the stoichiometric state in the 5×4 system and five extra holes in the 5×5 system, leading to the same hole concentration, 0.2/unit cell.

Figure 1 shows two kinds of vertical stripes in the system with 5×4 CuO_2 unit cells. In panel (a), the charged domain walls are shown running vertically along the copper sites (“site-stripe”). Spin is quenched along this stripe. Spins on other Cu sites are antiferromagnetically correlated with a π phase shift across the stripe, analogous to a one-dimensional domain wall. Due to e -ph interactions and accumulation of charge on the stripe, the oxygen sites adjacent to the stripe have pronounced lattice distortions and carry more charge density than other oxygen sites. In the stripe, the four oxygen ions around a copper ion distort asymmetrically between the direction along the stripe and that perpendicular to the stripe. In panel (b), the stripe is of zig-zag type and there is again an antiferromagnetic π phase shift across the stripe. Again, the lattice is strongly distorted for the oxygen sites adjacent to the stripe. Different from the site stripe, within the zig-zag stripe the four O ions around a Cu site are essentially equivalent and the stripe can be regarded as consisting of isolated CuO_4 clusters. This zig-zag stripe can be more stable than the vertical site stripe because of the greater number of relaxed oxygens. Figure 2(a) describes the spin-charge-lattice configuration of the diagonal-site stripe for the 5×5 system with the same parameters as above. In this stripe, the CuO_4 clusters are equivalent and, across the stripe, spins of the antiferromagnetic background again achieve an additional π phase shift. The HF energies of these striped phases are close (-4.77 , -4.83 , and -4.84 t_{pd} per unit cell for the vertical-site, zig-zag, and diagonal-site stripes, respectively). Al-

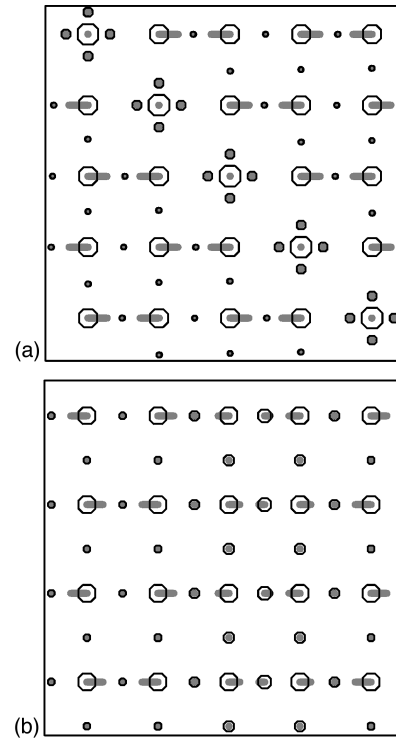


FIG. 2. Charge (radii of the circles) and spin (arrows) densities in the diagonal site stripe (a) and the oxygen-centered stripe (b). The symbols are as in Fig. 1. The hole concentration is 0.2.

though finite-system effect must be considered to correctly estimate the energy of larger systems, we emphasize that all these stripes are true local minima but dependent on boundary conditions (e.g., domains, dislocations, and twins in real materials). The on-site coupling β tends to stabilize zig-zag and diagonal stripes, and also to modulate charge density on vertical stripes. In fact, experimentally, both vertical and diagonal stripes have been observed. For example, vertical stripes are formed in doped La_2CuO_4 and diagonal stripes in doped La_2NiO_4 ,^{1,20} and current measurements cannot distinguish between vertical stripes of site or zig-zag type. Numerical DMRG calculations also predict that both the site and the zig-zag stripes are possible in a small cluster of the t - J model.¹² We expect that, because the stripes can also be formed with orientation perpendicular to those in Figs. 1 and 2, other more complicated patterns with crossed stripes are possible, analogous to, e.g., epitaxial surface discommensurations or fine-scale tweed. Local stripes of one kind can be defects on another kind of stripe and responsible for stripe melting,²¹ as we will discuss elsewhere. We have computed the HF electronic levels within the charge transfer gap for the various stripes, which will also be reported elsewhere. We do not describe here commensurate-incommensurate patterns or possible insulator-metal transitions within stripes, as a function of hole concentration.

All three stripes discussed above are centered on copper sites, whose spin is quenched. Recent data, e.g., neutron scattering measurements of the phonon behavior in the striped phase of $\text{La}_{1.85}\text{Sr}_{0.15}\text{CuO}_4$,¹⁴ indicate that the charge may be accumulating along an array of oxygen sites (i.e., Cu-Cu bond centered). In our three-band model, this oxygen stripe can indeed also exist. In Fig. 2(b), we show an oxygen stripe in the 5×4 system with a weaker e -ph coupling and a

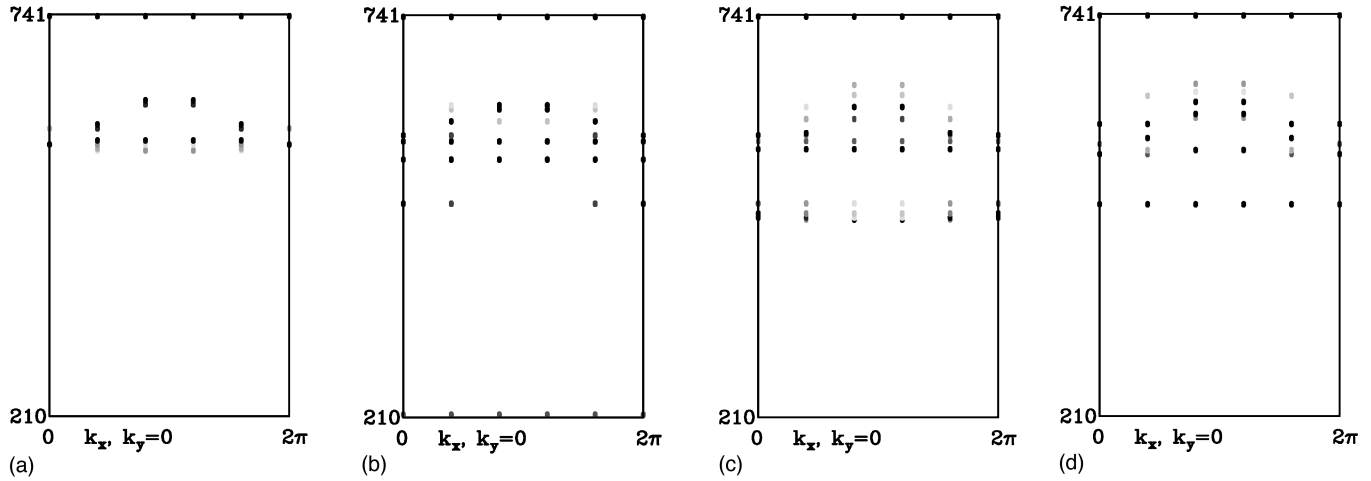


FIG. 3. Phonon dispersion in the undoped system (a), the vertical site striped phase (b), the vertical zig-zag striped phase (c), and the diagonal site striped phase (d). Points represent specific eigenmodes and their strength is proportional to the density of the mode. Frequencies in cm^{-1} .

smaller charge transfer gap $\Delta=2$, than for the above Cu-centered cases. Within the domain, the oxygen ions acquire much larger charge densities than those oxygen ions outside the stripe, and more importantly, they carry finite spin. Along the stripe, spins on oxygen are aligned antiparallel in the form of singlets. The coupling between the stripe (O) and environment (the adjacent Cu) is antiferromagnetic. Thus spins on copper sites at two sides of the stripe are parallel, showing that this stripe also gives an additional π phase shift to the antiferromagnetic background. Although from our small system calculations, strong e -ph couplings and direct oxygen-oxygen hopping tend to destabilize the oxygen stripe, we note that this stripe can be further stabilized by including a double-exchange interaction, or out-of-plane oxygen buckling, which are not included in model (1).

Having obtained the mean field spin-charge-lattice configurations, we carry out numerical random phase approximation (RPA) analysis of the phonon modes in these various striped phases. Figure 3 depicts the various phonon dispersions. Panel (a) is for the 5×5 undoped system, which is used for reference purposes. Panels (b)–(d) correspond to the vertical site stripe, the vertical zig-zag stripe, and the diagonal site stripe, respectively. Because of the formation of the stripes, some new phonon modes appear, generalizing the local phonon (“shape”) modes associated with individual localized charges (polarons).¹⁷ Lattice displacements both parallel and perpendicular to the stripes have been identified and should be valuable for experimentally distinguishing between types of stripes. Regarding the oxygen-centered stripe, in Fig. 4 we plot the phonon dispersion and the lowest mode at $\mathbf{k}=(\pi,0)$. The lattice configuration of this mode is the same as that of the recently observed ~ 70 meV phonon with momentum $(\pi,0)$ in $\text{La}_{1.85}\text{Sr}_{0.15}\text{CuO}_4$.¹⁴ According to the experiments, this mode is spatially localized, as is the lattice configuration of Fig. 4(b). This mode has frequency below the undoped oxygen breathing band, which is also consistent with the experimental data.

Since low-lying excitations will account for the low-temperature behavior, we also apply the RPA analysis to explore the spin and charge excitations and possible phonon resonances in the striped phases. Because of numerical con-

straints, we use a smaller system consisting of 3×4 unit cells for vertical stripes and a 3×3 system for diagonal stripes with hole concentration $1/3$. To understand the local magnetic structure, we focus on the spectral weight of magnetic excitations at $\mathbf{k}=(0,0)$. The spectral weight can be calculated as

$$f(\mathbf{k}, \omega) \propto \frac{\pi}{N_{\text{cell}}} \sum_{n \neq 0} |\langle 0 | \mathbf{S}_{\text{Cu}}^{\perp}(\mathbf{k}) | n \rangle|^2 \delta(\omega - (E_n - E_0)) \quad (2)$$

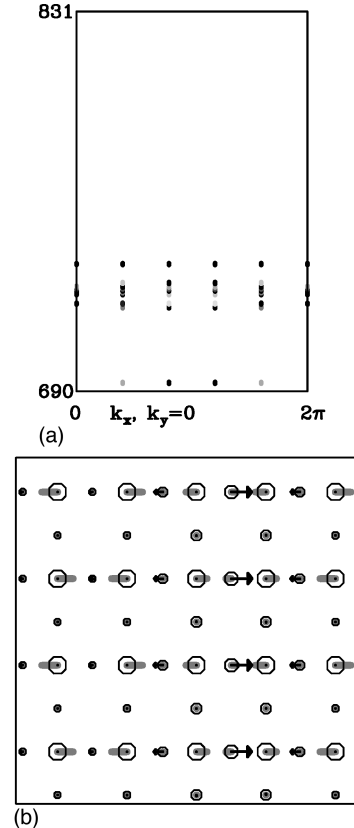


FIG. 4. (a) Phonon dispersion in the oxygen-centered stripe phase. The symbols are as in Fig. 3. (b) The lowest $(\pi,0)$ phonon mode in this stripe. The length of the arrow is proportional to the oxygen amplitude in this $(\pi,0)$ mode.

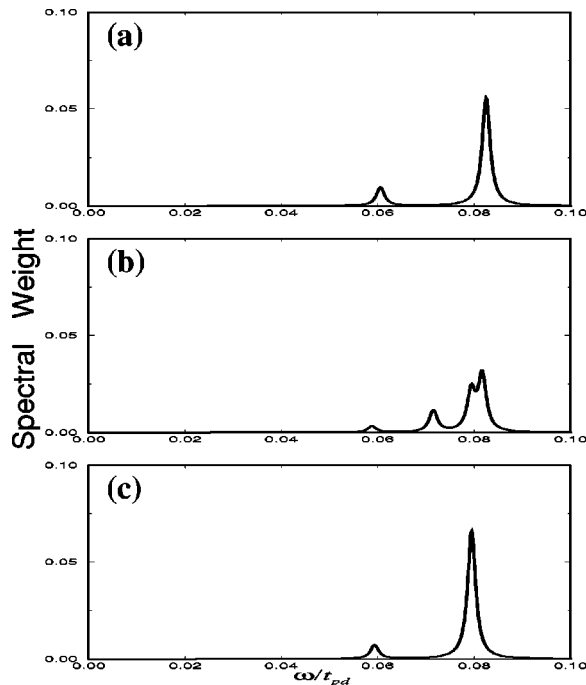


FIG. 5. Spectral weight of magnetic excitations in the vertical site stripe (a), vertical zig-zag stripe (b), and diagonal site stripe (c). The hole concentration is $1/3$.

for $\mathbf{k}=(0,0)$, $\mathbf{S}_{\text{Cu}}(\mathbf{k}) = \sum_{i \in \text{Cu}} \frac{1}{2} \sum_{\tau\tau'} c_{i\tau}^\dagger \sigma_{\tau\tau'} c_{i\tau'}$ with σ standing for Pauli matrices, the superscript \perp for the transverse components, and N_{cell} for the number of CuO_2 units. Figure 5 shows the low-energy magnetic excitation spectral weights for the vertical site stripe (a), the vertical zig-zag stripe (b), and the diagonal site stripe (c). In these stripes, there are some intense low-energy magnetic excitations localized around the magnetic *edges* of the stripes, and with energies coinciding with the stripe phonon band. The detailed structure of these excitations depends on the type of stripe, but they typically have a local spin-wave character with the local magnetic coupling modulated by the oxygen pattern around the stripe. For example, the vertical zig-zag stripe has one more low-energy mode than the site stripe. This difference may be useful to experimentally distinguish between stripes.

The spectral weights of charge excitations also show some modes in the phonon energy range, though their intensity is much weaker than that in the spin channel. Our calculations for spin excitation spectral weight with different momenta indicate that in these stripes, the peak of the strong antiferromagnetic spin-spin correlation is split or shifted from zero energy to a small but finite energy. This finite energy excitation may be related to a spin pseudogap in disordered/meandering stripes, but larger systems (smaller momenta) are necessary for the assignment.

In summary, using a two-dimensional three-band Peierls-Hubbard model, we find that several kinds of stripes can exist (at least as global metastable configurations): the vertical site stripe, the vertical zig-zag stripe, the diagonal site stripe, and the oxygen-centered (bond) stripe. In all these stripes, spins on copper sites receive a π phase shift across the stripe. Due to the formation of the stripe, some new local phonon modes appear. These different kinds of stripes may be realized in different materials. For example, vertical stripes are observed in doped La_2CuO_4 and diagonal stripes in doped La_2NiO_4 .^{1,20} The zig-zag stripe we identified may be relevant to ladder materials as well as layered cuprates.²² Recent neutron scattering measurements indicate that the oxygen-centered stripe is formed in $\text{La}_{1.85}\text{Sr}_{0.15}\text{CuO}_4$ and a softened phonon with energy ~ 70 meV has been observed.¹⁴ Our theoretical calculations predict a local (shape) mode in the oxygen-centered stripe with the correct symmetry and lying below the undoped oxygen breathing band. We also calculated the spectral weight of magnetic and charge excitations for different stripes and find the possibility of spin-phonon and weaker charge-phonon resonances. Detailed experimental study of dynamical spin-phonon correlations, correlated with electronic gap signatures, will be helpful for understanding the signatures of stripes. Estimates of pairing fluctuations in the presence of the various stripes (especially oxygen-centered) are in progress.

We are grateful to K. Yonemitsu for important consultations on the RPA code, and to T. Egami, P. C. Hammel, R. L. Martin, M. Salkola, S. A. Trugman, Y. Yoshinari, and J. Zaanen for helpful discussions. This work was supported by the U.S. Department of Energy.

¹J. M. Tranquada *et al.*, Nature (London) **375**, 561 (1995).

²J. M. Tranquada *et al.*, Phys. Rev. Lett. **78**, 338 (1997).

³V. J. Emery and S. A. Kivelson, Physica C **209**, 597 (1993); Nature (London) **374**, 434 (1995).

⁴S. A. Kivelson and V. J. Emery, in *Strongly Correlated Electronic Materials: The Los Alamos Symposium 1993*, edited by K. S. Bedell *et al.* (Addison-Wesley, Reading, 1994).

⁵A. H. Castro Neto and D. Hone, Phys. Rev. Lett. **76**, 2165 (1996).

⁶Yu. A. Krotov, D. H. Lee, and A. V. Balatsky, Phys. Rev. B **56**, 8367 (1997).

⁷J. Zaanen, M. L. Horbach, and W. van Saarloos, Phys. Rev. B **53**, 8671 (1996).

⁸J. A. Vergés, E. Louis, P. S. Lomdahl, F. Guinea, and A. R. Bishop, Phys. Rev. B **43**, 6099 (1991).

⁹D. Poilblanc and T. M. Rice, Phys. Rev. B **39**, 9749 (1989).

¹⁰J. Zaanen and O. Gunnarsson, Phys. Rev. B **40**, 7391 (1989).

¹¹M. Inui and P. B. Littlewood, Phys. Rev. B **44**, 4415 (1991).

¹²S. R. White and D. J. Scalapino, cond-mat/9705128, Phys. Rev. Lett. (to be published).

¹³J. Zaanen and P. B. Littlewood, Phys. Rev. B **50**, 7222 (1994); A. Bianconi *et al.*, Phys. Rev. Lett. **76**, 3412 (1996).

¹⁴T. Egami *et al.* (unpublished).

¹⁵P. Wochner *et al.* (unpublished); P. C. Hammel *et al.* (unpublished).

¹⁶W. Reichardt *et al.*, Physica C **162**, 464 (1989).

¹⁷K. Yonemitsu, A. R. Bishop, and J. Lorenzana, Phys. Rev. Lett. **69**, 965 (1992); Phys. Rev. B **47**, 12 059 (1993).

¹⁸Z. G. Yu, A. R. Bishop, and J. T. Gammel (unpublished).

¹⁹M. S. Hybertsen, M. Schlüter, and N. E. Christensen, Phys. Rev. B **39**, 9028 (1989).

²⁰J. M. Tranquada *et al.*, Phys. Rev. Lett. **73**, 1003 (1994).

²¹H. E. Viertiö and T. M. Rice, J. Phys.: Condens. Matter **6**, 7091 (1994).

²²E. Dagotto and T. M. Rice, Science **271**, 618 (1996).